Theoretical Study on the Reaction of Butadiynyl Radical (C_4H) With Ethylene (C_2H_4) to Form C_6H_4 and H

JOONGHAN KIM, HYOTCHERL IHEE

Department of Chemistry, Center for Time-Resolved Diffraction, Graduate School of Nanoscience and Technology (WCU), KAIST, Daejeon 305-701, Republic of Korea

ABSTRACT: The reaction mechanisms of the butadiynyl radical (C_4H) with ethylene (C_2H_4) to form H and C_6H_4 via hydrogen elimination are investigated using the density functional theory and high-level ab initio methods. The calculated geometrical parameters and dipole moment of the $^2\Pi$ state of C_4H are in excellent agreement with previously reported values using CCSD(T) with large basis sets. The calculated reaction enthalpy is also in excellent agreement with that of previously reported value. These results indicate that theoretical level in this work is optimal and more expensive calculations may not be necessary for the systems studied in this work. Eight isomers of C_6H_4 are considered in this work, and we present the highly complex reaction pathways by grouping them into three categories; (i) pathways including only chain intermediates without any ring components, (ii) pathways including ring formations except the six-membered ring, and (iii) pathways including the six-membered ring. On the basis of the calculated results, the most favorable reaction pathway is simple and found in the first category; H elimination from the initial chain adduct of C_4H with C_2H_4 yields H and one of C_6H_4 isomers ($CH_2{=}CH{-}C{\equiv}C{-}C{\equiv}CH$). This reaction is similar to that of the reaction of ethynyl (C_2H) radical with C_2H_4. This result clarifies the assumption in the recent experimental kinetics study. ©2011 Wiley Periodicals, Inc. Int J Quantum Chem 112: 1913–1925, 2012

Key words: density functional theory; ab initio; radical; reaction mechanism; astrochemistry

Introduction

$\mathbf{T}$he butadiynyl radical, C_4H (CCCCH), was first observed in 1975 in low-temperature argon and neon matrices after the UV photolysis of C_4H_2 (diacetylene) [1]. It also was detected in 1978 in the interstellar medium [2]. Experimental and theoretical investigations for this kind of unusual hydrocarbon (or hydrogen-deficient) compounds are important not only for combustion chemistry (because of long chain of C_4H, it can be crucial role for the formation of soot) but also for better understanding the chemistry of the interstellar medium and planetary atmospheres. Despite numerous theoretical investigations of the reactions involving ethynyl (C_2H) radical [3–8], which is also considered as a precursor to polycyclic aromatic hydrocarbons such as C_4H, a theoretical study for the reaction involving C_4H is still lacking. We found only one theoretical study for the reaction of C_4H with C_2H_2 [5]. On the other hand, experimental investigations for C_4H with various saturated and unsaturated hydrocarbons using the pulsed laser photolysis have been recently reported [9, 10]. The rate coefficients for these reactions have been provided, but their detailed reaction mechanisms are still unknown. Therefore, a theoretical investigation for unraveling detailed reaction mechanism of the reaction involving C_4H radical is urgently demanded. In addition, thorough understanding of this reaction can provide insight for reaction mechanisms involving radical species in general and assist further experimental effort using various spectroscopic and structural probes [11–19].

In the present work, we have investigated the reaction of C_4H with C_2H_4 using the density functional theory (DFT) and high-level ab initio methods. The plausible reaction mechanisms are proposed. Moreover, we propose the most favorable reaction pathway according to our calculated results. This pathway coincides with the one that was assumed to be the most favorable reaction pathway in recent experimental study for the $C_4H + C_2H_4$ reaction [9]. To our best knowledge, this is the first instance to study the reaction of C_4H with C_2H_4 theoretically.

Computational Details

The molecular geometries and harmonic vibrational frequencies were calculated using DFT [20,

21]. The M06-2X functional (hybrid-meta) [22] was used for calculations on the reaction of C_4H with C_2H_4 (ethylene). The $6\text{-}311\text{++}G(d,p)$ basis sets were used for all atoms. The coupled-cluster singles and doubles method including a perturbative estimate of triples (CCSD(T)) [23] with the $6\text{-}311\text{++}G(2df,2pd)$ basis sets was used to obtain more accurate energies for all species. All CCSD(T)/$6\text{-}311\text{++}G(2df,2pd)$ single-point calculations were performed at the geometries optimized by M06-2X/$6\text{-}311\text{++}G(d,p)$ level, and all energies were reported with the zero-point energy (ZPE) corrections (CCSD(T)/$6\text{-}311\text{++}G(2df,2pd)$//M06-2X/$6\text{-}311\text{++}G(d,p)$). The ZPE values of M06-2X/$6\text{-}311\text{++}G(d,f)$ level were used for the ZPE corrections in CCSD(T) single-point calculations. All transition states presented in this work were identified by one imaginary frequency and confirmed by using the intrinsic reaction coordinate method [24, 25]. We also used the natural population analysis (NPA) [26] for characterizing atomic charges and electronic structures. All calculations were performed using the Gaussian09 program [27]. We considered only the doublet spin states of C_6H_5 ($C_4H + C_2H_4$), namely, other spin states were not considered in this work. Spin contaminations of all radical species are negligible because the $\langle S^2 \rangle$ values of all species are close to the exact value for the doublet (0.75).

Results and Discussion

In this article, we used the notations of IMn and TSn-m for the intermediate n (IM) and the transition state between the IMn and the IMm, respectively. The "Pj" means the product j and its spin multiplicity is the singlet. The "TSj-Pk" indicates the transition state between the IMj and the Pk. The spin multiplicity of all IMs and transition states (TSs) is the doublet. Although both M06-2X/$6\text{-}311\text{++}G(d,p)$ and CCSD(T)/$6\text{-}311\text{++}G(2df,2pd)$ energies with ZPE corrections on the reaction PESs are summarized in Table I, only CCSD(T) energies are used for the discussion, because CCSD(T) provides more reasonable thermochemical energy values. Two isolated reactant molecules ($C_4H + C_2H_4$ in Fig. 1) were used to define reference energy (0.0 kcal/mol) on all reaction PESs. That is, all energy values are relative to the reference energy. We found eight possible products (C_6H_4, from P1 to P8 in Fig. 1) via H elimination

TABLE I

The relative energies (in kcal/mol) including ZPE correction of all species calculated by
M06–2X/6–311++G(d,p) and CCSD(T)/6–311++G(2df,2pd)//M06–2X/6–311++G(d,p).

Species	M06–2X	CCSD(T)	Species	M06–2X	CCSD(T)
IM1	−59.7	−58.8	IM17	−15.8	−8.5
TS1-P1	−22.8	−21.5	TS17–18	−7.8	−2.4
TS1–2	−20.2	−15.9	IM18	−59.5	−53.8
TS1–5	−28.9	−25.3	TS18-P5	1.5	8.0
IM2	−68.6	−65.1	P5 + H	−1.9	5.2
TS2-P1	−23.6	−21.5	TS10–12	−20.6	−21.4
TS2–6	−64.3	−62.7	IM12	−57.8	−55.6
IM5	−76.7	−73.8	TS12–13	−24.4	−20.0
TS5-P1	−26.5	−24.9	TS6–23	16.8	16.0
TS5–6	2.8	5.4	IM23	−2.0	1.1
IM6	−70.8	−67.4	TS23–13	7.7	11.1
TS6-P1	−24.4	−22.0	IM13	−74.8	−71.9
P1 + H	−29.1	−29.3	TS13-P4	−13.1	−11.7
TS1–3	−59.5	−58.5	P4 + H	−17.5	−15.9
IM3	−59.1	−58.0	TS2–19	−30.6	−26.5
TS3–4	−46.4	−42.6	IM19	−59.0	−61.0
IM4	−57.9	−51.3	TS19-P6	−31.5	−32.8
TS3–33	0.9	1.8	TS2–20	−32.4	−33.5
IM33	−31.3	−32.5	IM20	−59.1	−56.2
TS33–34	4.3	4.1	TS20–21	−18.6	−15.1
IM34	−11.3	−11.1	IM21	−59.6	−56.1
TS34–7	−4.3	−3.4	TS21–22	−52.7	−50.9
IM7	−34.9	−32.4	IM22	−123.3	−118.8
TS7–16	−1.8	4.0	P6 + H	−38.3	−40.4
IM16	−26.2	−22.4	TS2–24	−19.3	−16.3
TS16-P2	32.2	37.2	IM24	−68.9	−67.4
P2 + H	29.0	32.9	TS24–25	−24.6	−23.4
TS3–9	−19.7	−20.0	IM25	−45.5	−44.0
IM9	−50.3	−48.3	TS25–26	−43.6	−43.0
TS9–10	−18.2	−17.9	IM26	−56.0	−49.6
IM10	−68.0	−67.1	TS26-P7	−26.3	−19.4
TS10–11	−33.2	−31.8	P7 + H	−31.7	−25.1
IM11	−43.3	−39.0	TS24–27	−26.8	−24.5
P3 + H	31.2	35.2	IM27	−26.1	−23.7
TS13–14	−6.4	−2.3	TS27–28	−23.4	−22.4
IM14	−9.1	−3.7	IM28	−23.0	−22.0
TS14–15	1.1	7.0	TS28–29	−19.9	−19.4
IM15	−53.9	−48.9	IM29	−20.9	−20.1
TS15-P5	2.8	10.3	TS29–30	−20.5	−18.6
TS3–35	12.8	12.2	IM30	−40.7	−37.9
IM35	−4.0	−8.8	TS30–31	−0.8	0.3
TS35–36	−2.9	−0.2	IM31	−31.1	−28.7
IM36	−3.7	0.2	TS31–32	−7.5	−3.6
TS36–8	−2.3	−0.6	IM32	−44.7	−43.2
IM8	−3.8	−2.2	TS32-P8	−9.9	−4.5
TS8–17	35.6	37.6	P8 + H	−14.8	−9.0

($C_4H + C_2H_4 \rightarrow C_6H_4 + H$). Although other products channels may be possible, we have focused on the H elimination. Even for this single type of reaction, the reaction pathways are highly complex. For the sake of discussion and clear presentation, we classified the pathways as in the following sections.
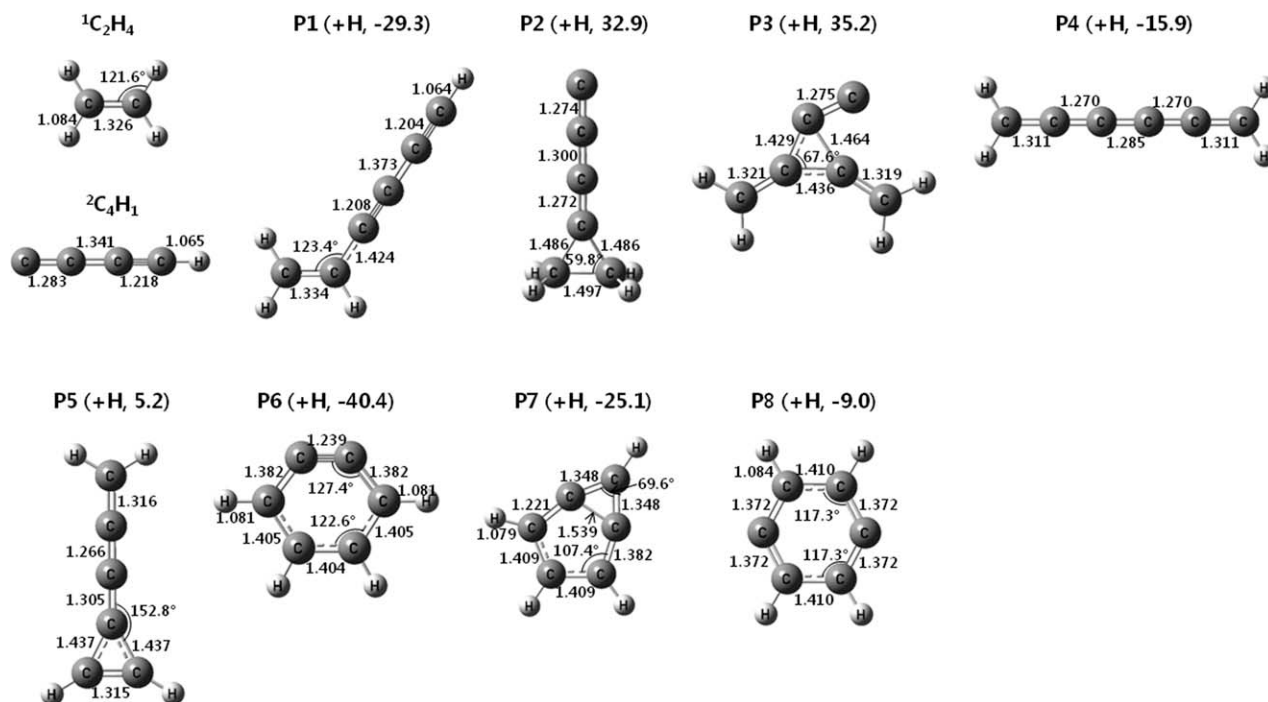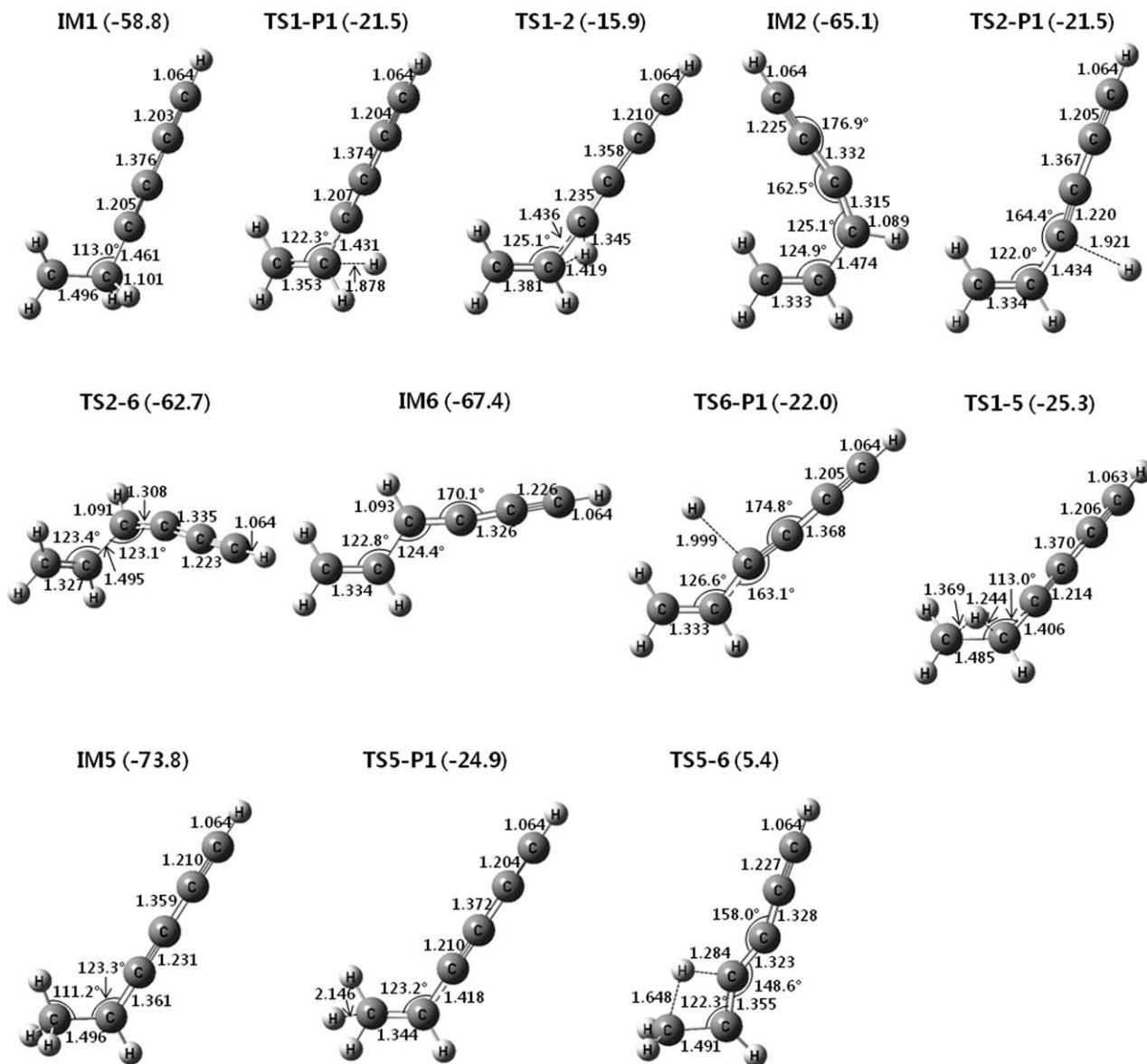
FIGURE 1. Selected parameters (bond lengths in Å and angles in degrees) of optimized structures of the reactants (C_2H_4 and C_4H) and all products (from P1 to P8) calculated by M06-2X/6-311++G(d,f). The energy of C_4H with C_2H_4 is set to 0.0 kcal/mol as a reference energy. Values in parentheses are the relative energies (in kcal/mol) calculated by CCSD(T)/6-311++G(2df,2pd)//M06-2X/6-311++G(d,f).

PATHWAYS INCLUDING CHAIN IMs (NO RINGS)

As noted above, all reactants and candidate products are depicted in Figure 1 and all optimized IMs and transition states structures and the reaction PESs for the pathways including chain IMs (no rings) are depicted in Figures 2 and 3, respectively. The geometrical parameters of linear C_4H ($^2\Pi$) are shown in Figure 1. The other electronic state, $^2\Sigma^+$, of C_4H lies slightly higher in energy (0.76 kcal/mol) than $^2\Pi$ state at M06-2X/6-311++G(d,p) level of theory (moreover, the $^2\Sigma^+$ state of C_4H is not a local minimum, namely, it has two imaginary frequencies). As the different theory level applied in calculations for C_4H gives a different ground state, the controversy about true electronic ground state of C_4H still remains [28–31]. Recent calculations for C_4H using CCSD(T)/aug-cc-pVQZ method, quite expensive calculation, has given that $^2\Sigma^+$ state of C_4H is the ground state, but the energy difference between $^2\Sigma^+$ and $^2\Pi$ state is 0.000041 hartree, 0.026 kcal/mol [30]. Our result differs. However, in real situation, both electronic states may be populated simultaneously due

to extremely small energy difference, and therefore, the effect on the reactions of C_4H with C_2H_4 is negligible. Despite of the mismatch of the ground state between our calculated result and recent CCSD(T) result, the geometrical parameters (1.283, 1.341, 1.218, and 1.065 Å, see Fig. 1) and dipole moment (4.5274 Debye) of the $^2\Pi$ state of C_4H calculated by M06-2X/6-311++G(d,p) are in excellent agreement with those (1.295, 1.342, 1.226, and 1.065 Å and 4.3336 Debye, see Table 2 in Ref. [30]) calculated by CCSD(T)/aug-cc-pVQZ [30]. Thus, one can conclude that M06-2X/6-311++G(d,p) gives reasonable results for the reaction PESs. The previous study, which investigated other isomers of C_4H, reported that linear isomer is a ground state of C_4H (C1C2C3C4H) [32], and other isomers of C_4H have not been considered in this work. The NPA charges of C atoms of C_4H (C1C2C3C4H, $^2\Pi$) calculated by NPA are +0.127, −0.230, −0.101, −0.034 from C1 to C4 (cf. the NPA charges of the $^2\Sigma^+$ state are as follows; +0.310, −0.313, −0.114, −0.117, they are similar to those of the $^2\Pi$ state. Therefore, the same discussion can be applied if the reactions are initiated from the $^2\Sigma^+$ state of C_4H). Each of both C atoms

FIGURE 2. Selected parameters (bond lengths in Å and angles in degrees) of optimized structures of the transition states and the intermediates calculated by M06-2X/6-311++G(d,f) on reaction PESs of the pathways including chain intermediates (no rings). Values in parentheses are the relative energies (in kcal/mol) calculated by CCSD(T)/6-311++G(2df,2pd)//M06-2X/6-311++G(d,f).

in C_2H_4 has charge of -0.372. This result indicates that the terminal C1 atom of C_4H, whose charge is 0.127, can be readily attached to the C atom of C_2H_4, whose charge is -0.372. [It is noteworthy that the charges the $^2\Pi$ state of C_4H calculated by the Mulliken population analysis (MPA) are -0.433, $+0.144$, $+1.869$, and -1.753 from C1 to C4. These values are substantially different from those calculated by NPA in the order and magnitude of charges, indicating that MPA is an improper method to calculate atomic charges for this kind of species.]

As shown in Figure 2, the C1 atom of the linear C_4H can attach to one of C atoms of C_2H_4, resulting in IM1. The relaxed PES scan calculation between C1 of C_4H and one of C atom in C_2H_4 shows that this process is barrierless, indicating that the IM1 is the initial adduct. The IM1 is directly connected to the P1 through the transition state, TS1-P1, via H elimination. A similar result
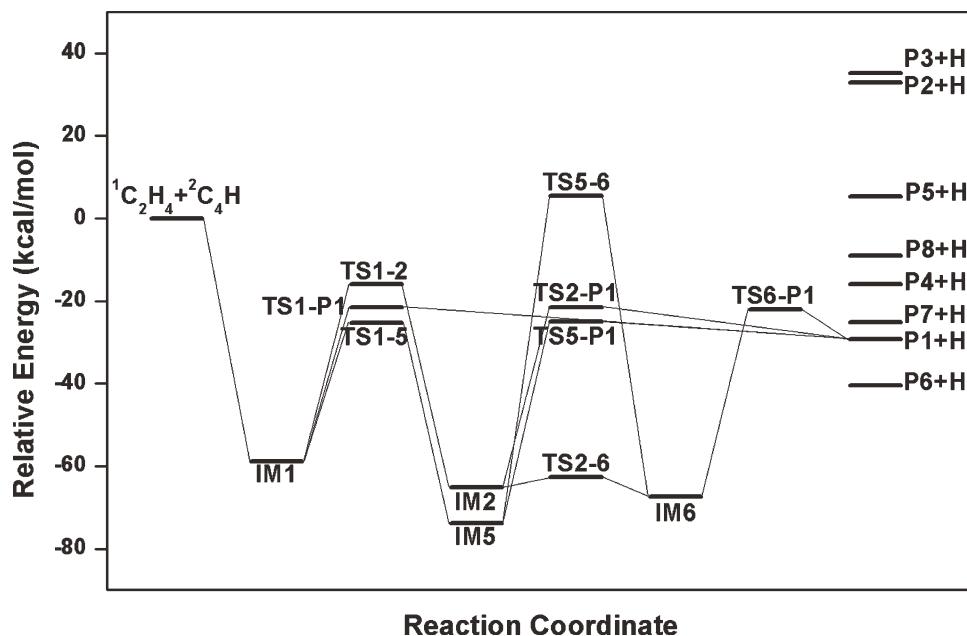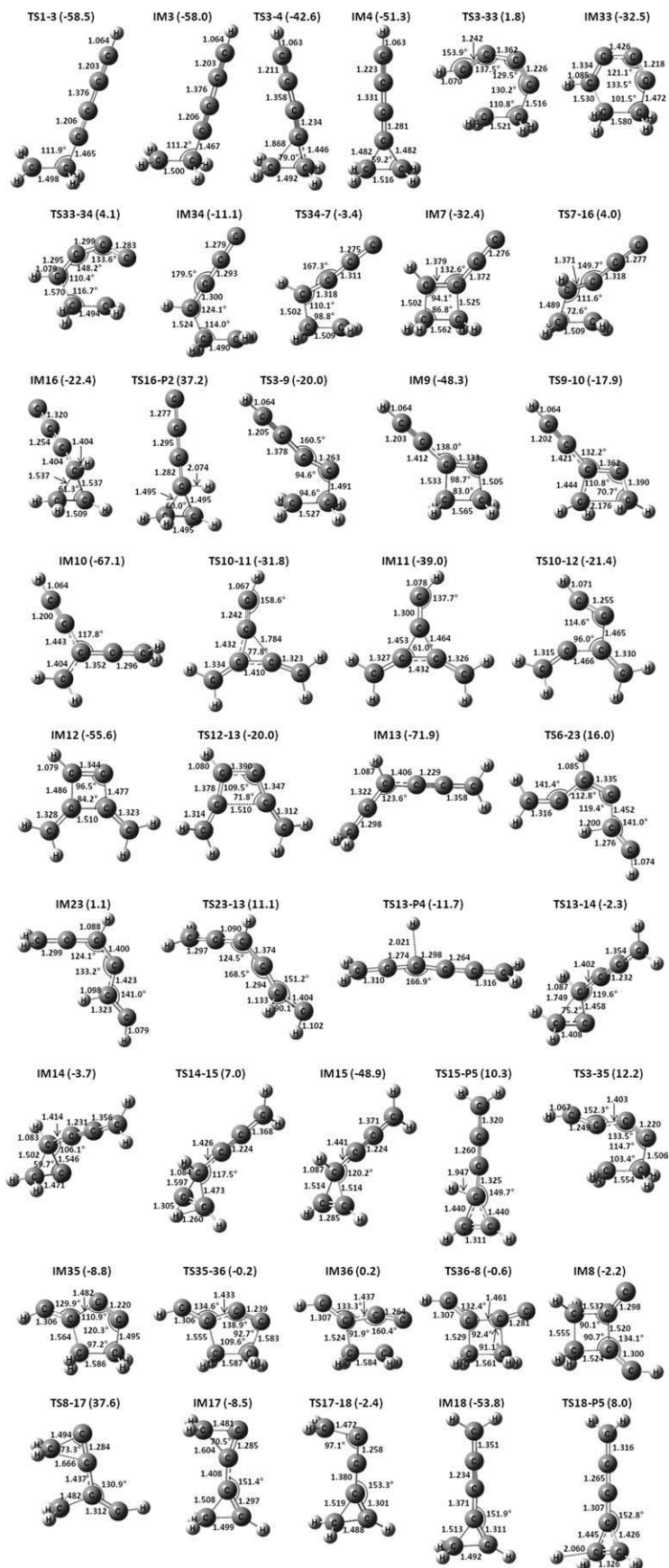
FIGURE 3. Reaction PESs of the pathways including chain intermediates (no rings) calculated by CCSD(T)/6-311++G(2df,2pd)//M06-2X/6-311++G(d,f). The related optimized structures are shown in Figure 2.

is found in the $C_2H + C_2H_4$ reaction [4]. Alternatively, one H atom of the ethylene moiety of IM1 can migrate to C1 atom of the C_4H moiety, thereby forming IM2. The bridged H between two carbon atoms is clearly seen in the TS1-2. The shape of the IM2 is a *cis*-like structure with respect to the positions of two H atoms attached to the second and third C atoms from left. A *trans*-like structure, IM6, can form through the rotational transition state, TS2-6. Both IM2 and IM6 are also connected to the P1 through the transition states (TS2-P1 and TS6-P1) of the H elimination. The H atom of the ethylene moiety of IM1 can take another migration route to form IM5 that has a terminal methyl group. The IM5 possesses the lowest relative energy (-73.8 kcal/mol, see Table I) among IMs belonging to this reaction pathway. The IM5 is connected to the IM6 through the TS5-6, but with a high barrier (68.4 kcal/mol). Again the four IMs (IM1, IM2, IM5, and IM6) are directly linked to the P1 through the four transition states (TS1-P1, TS2-P1, TS5-P1, and TS6-P1) via H elimination. Among these transition states, the barrier of the TS1-P1 (37.3 kcal/mol, see Table I) is the smallest, indicating that this reaction pathway is likely the most favorable reaction pathway. We will return to this in a later section (section 4). It should be noted that all these processes in this reaction pathway are quite similar to those of the reaction of C_2H with C_2H_4 [4].

The reaction enthalpy ($C_4H + C_2H_4 \rightarrow C_6H_4$ (P1) + H) calculated by CCSD(T)/6-311++G(2df,2pd)// M06-2X/6-311++G(d,f) is -121.3 kJ/mol, which is in excellent agreement with the previous estimated value (-124 kJ/mol) using CCSD(T) with complete basis set (CBS) limit, a quite expensive calculation, as well as values from the NIST-CCCBD (Computational Chemistry Comparison and Benchmark Database) [9]. This excellent agreement supports that the theoretical level in this work is optimal in a cost-effective manner.

PATHWAYS INCLUDING RING FORMATION (EXCEPT SIX-MEMBERED RING)

All optimized structures and the reaction PESs for the pathways including ring formation (except six-membered ring) are depicted in Figures 4 and 5, respectively. In this section, the pathways including the formation of the ring except a six-membered ring are discussed. The formations of a six-membered ring will be discussed in the next section (see section 3). As can be seen in Figure 4, the CH_2 unit rotates in TS1-3 and the IM3 forms. We also performed the relaxed PES scan calculation for the IM3 to verify the existence of the barrier. The calculated result shows that the IM3 can form as an initial adduct of the $C_4H + C_2H_4$ reaction via barrier-less process. The reaction PES in

FIGURE 4. Selected parameters (bond lengths in Å and angles in degrees) of optimized structures of the transition states and the intermediates calculated by M06-2X/6-311++G(d,f) on reaction PESs of the pathways including ring formation (except six-membered ring). Values in parentheses are the relative energies (in kcal/mol) calculated by CCSD(T)/6-311++G(2df,2pd)//M06-2X/6-311++G(d,f).
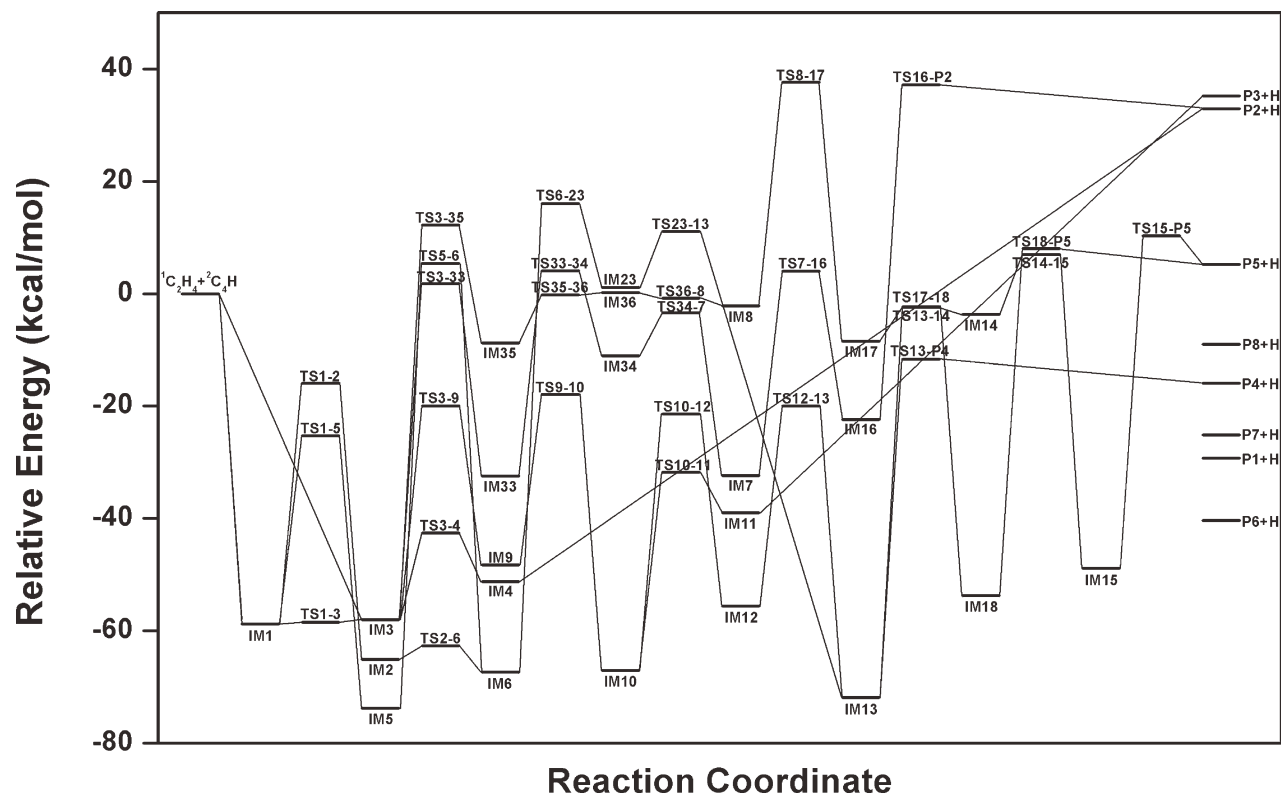
FIGURE 5. Reaction PESs of the pathways including ring formation (except six-membered ring) calculated by CCSD(T)/6-311++G(2df,2pd)//M06-2X/6-311++G(d,f). The related optimized structures are shown in Figure 4.

Figure 5 shows odd behavior that the energy of the TS1-3 is lower than the IM3. This indicates that the rotation of CH_2 unit may be a barrier-less process or has quite small barrier energy. This can be identified by the magnitude of the transition mode of the TS1-3, -171.6 cm^{-1}; it is a very small value. The rotated CH_2 unit attracts one of the neighboring C atoms of IM3 as can be seen in the TS3-4 and a bridged structure, IM4 forms (the IM4 is not an initial adduct between C_4H and C_2H_4, because the relaxed PES scan calculation of the IM4 shows a barrier). P2 can be formed from IM4 via H elimination. The P2 lies much higher in energy than the P1 due to the ring strain of a three-membered ring. As shown in all reaction PESs, the three products (P2, P3, and P5) that have a three-membered ring lie much higher in energy than other products. In addition, they possess positive relative energies. The reaction pathways leading to these products are likely to be unfavorable.

As shown in Figure 4, the IM7, IM8, and IM9 look like initial adducts involving a four-membered ring through direct interaction between two

C atoms of C_4H and both C atoms of C_2H_4 without barrier. However, all three IMs are not initial adducts, based on the existence of a barrier during the relaxed PES scan calculations. All the three IMs form through ring closing process from IM3 (see Fig. 4). These results are different from those found in the C_2H + C_2H_4 reaction where the direct interaction two C atoms of C_2H and both C atoms of C_2H_4 makes an initial adduct with a four-membered ring (C_4H_5, see q2 structure in Figure 1 in Ref. [4]). Rather long chain of C_4H may distort the PES and cause the different reaction step. However, it is worth noting that the relative energy order of these three IMs can be expected by NPA charges of C_4H and C_2H_4 (see section 1, where the NPA charges have been already shown). Only the terminal C atom (C1) of C_4H (C1C2C3C4H) has positive charge ($+0.127$). It can be expected that attaching two C atoms (C1 and C2) to the two negatively charged C atoms in C_2H_4 (IM9) is preferable. In contrast, attaching two middle C atoms (C2 and C3) of C_4H, which have large negative charges to the two negatively charged C atoms in C_2H_4 (IM8), is likely to be

undesirable. The IM7, where C3 and C4 are attached to the C atoms of C_2H_4, lies between the IM9 and IM8 due to less negatively charged C atoms (C3 and C4). Indeed, the IM9 possesses the lowest relative energy (-48.3 kcal/mol, see Table I) and the IM8 (-2.2 kcal/mol, see Table I) lies higher in energy than the IM7 (-32.4 kcal/mol, see Table I) and IM9. Such attachment on both C atoms of C_2H_4 makes the C—C bond length of C_2H_4 elongated because electrons occupy an antibonding orbital of C_2H_4. As shown in Figure 4, all C—C bond length of C_2H_4 moiety in IM7, IM8, and IM9 are around 1.56 Å, longer than that of C_2H_4 (1.326 Å).

The ring closing process of the IM3 forms the IM33 involving a five-membered ring through the TS3-33. This process requires high reaction barrier (59.8 kcal/mol) due to the rolling up of the long chain. The ring opening process of the opposite part of the ring closing occurs in the TS33-34 and the IM34 forms. Making four-membered ring through the TS34-7 yields the IM7. The ring opening of the IM7 follows through the TS7-16, and subsequently, a three-membered ring forms in the IM16. The H atom on the three-membered ring is detached through the TS16-P2 and leads to the P2. This process is unfavorable due to high reaction barrier (59.6 kcal/mol, see Table I).

The IM9 can form through a ring closing of the IM3 via the TS3-9. Through a ring opening process via TS9-10 (as in the TS7-16), the reaction proceeds to the IM10. In the IM10, the reaction pathway branches to TS10-11 and TS10-12 through a ring closing process. The IM11 forms by making a three-membered ring. The reaction finally proceeds to the P3 that lies high in energy due to the three-membered ring strain. In contrast, the IM12 forms through making a four-membered ring. The IM12 lies lower in energy than the IM11 due to less ring strain. The very stable chain IM, IM13, forms through a ring opening via the TS12-13. The IM13 can also form from the IM6, which participates in the previous reaction pathway (see Pathways Including Chain IMS (No Rings) section). One of *trans* H atoms migrates to another C atom in the TS6-23. The migrated H atom continuously moves to the terminal C atom (CH group) via TS23-13, finally leading to the IM13. However, this process may not be feasible because of too high barrier (83.4 kcal/mol, see Table I) between the IM6 and TS6-23. The IM13 is connected to the chain product, P4, through the H elimination. The P4 lies low in

energy due to the absence of the ring strain. In addition, the IM13 can be a starting point leading to another product, P5. As can be seen in Figure 4, a three-membered ring forms through the TS13-14. In the TS14-15, one H atom of CH_2 of the three-membered ring moves to next C atom of the three-membered ring. The H atom is detached on the C atom of three-membered ring in the TS15-P5 and leads to the P5.

As shown in Figure 5, the reaction PES from the IM8 also leads to the P5. The IM8 forms through similar process of forming the IM7. First, the ring-closing process from the IM3 takes place via the TS3-35. Subsequently, the ring-opening process occurs through the TS35-36. The terminal C atom (C1 of C_4H) moves in TS36-8 and the IM8 forms. This process also shows odd behavior that both TS35-36 and TS36-8 lie below in energy than the IM8, as in TS1-3 and IM3. This also indicates that the terminal C atom (C1 of C_4H) can freely move. The C—C bond of C_2H_4 breaks and a ring-opening process takes place in the TS8-17. In the IM17, two three-membered rings form. The one three-membered ring is open, and it leads the IM18. Finally, the P5 forms via H elimination. Numerous reaction pathways lead to the P5, but these reactions are not feasible due to too high reaction barriers.
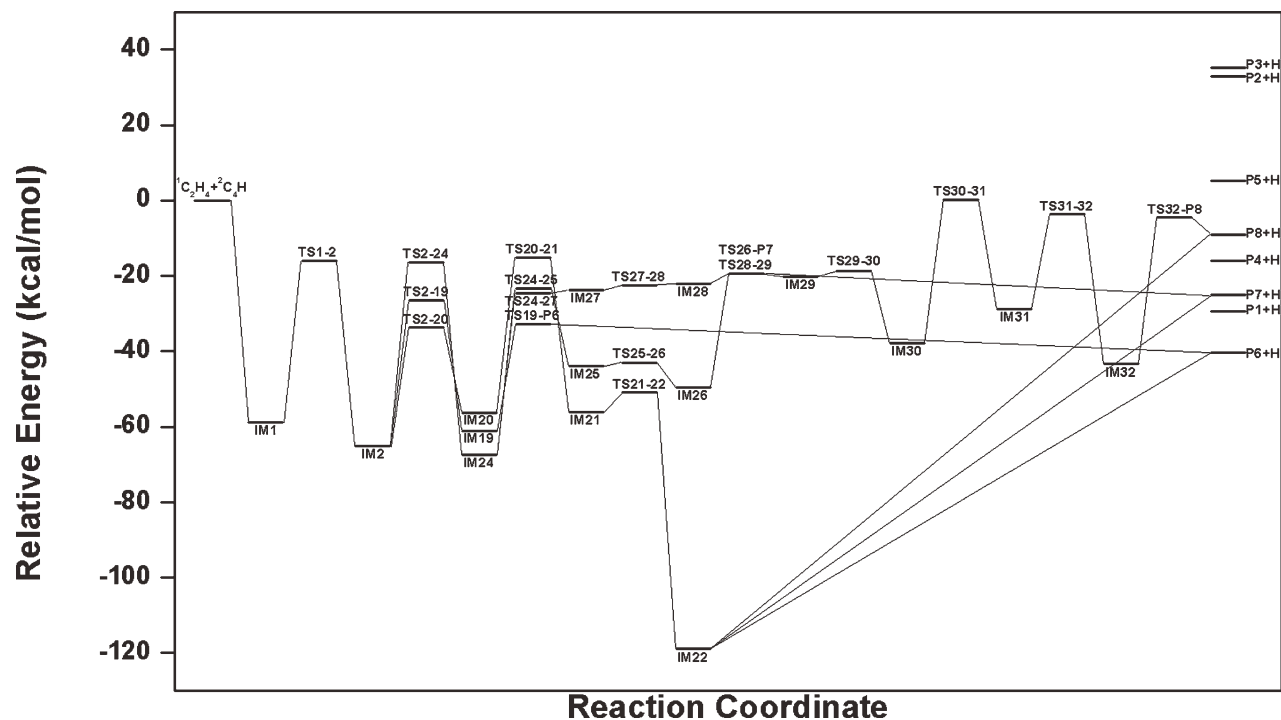
PATHWAYS INCLUDING FORMATION OF SIX-MEMBERED RING

All optimized structures and the reaction PESs for the pathways including formation of six-membered ring are depicted in Figures 6 and 7, respectively. C_4H with C_2H_4 has an enough number of C atoms to form a six-membered ring unlike C_2H with C_2H_4, and these possibilities are investigated in this work. Six-membered ring closings are initiated from the IM2, a *cis*-like structure (see Fig. 2). Because of the possession of *cis* position in the IM2, the distance between two terminal C atoms is closer than that of the IM6, a *trans*-like structure (see Fig. 2). Thus, it makes the IM2 form a six-membered ring easily. We have tried to find ring closings from the IM6, but no transition states have been found.

The direct ring closing occurs through the TS2-19, and the H elimination from the IM19 leads to the P6. The P6 has another formation route that involves H atom transfer in the TS2-20. The IM20 goes through the *cis-trans* isomerization in the TS20-21 to form the IM21. As shown in Figure 6,
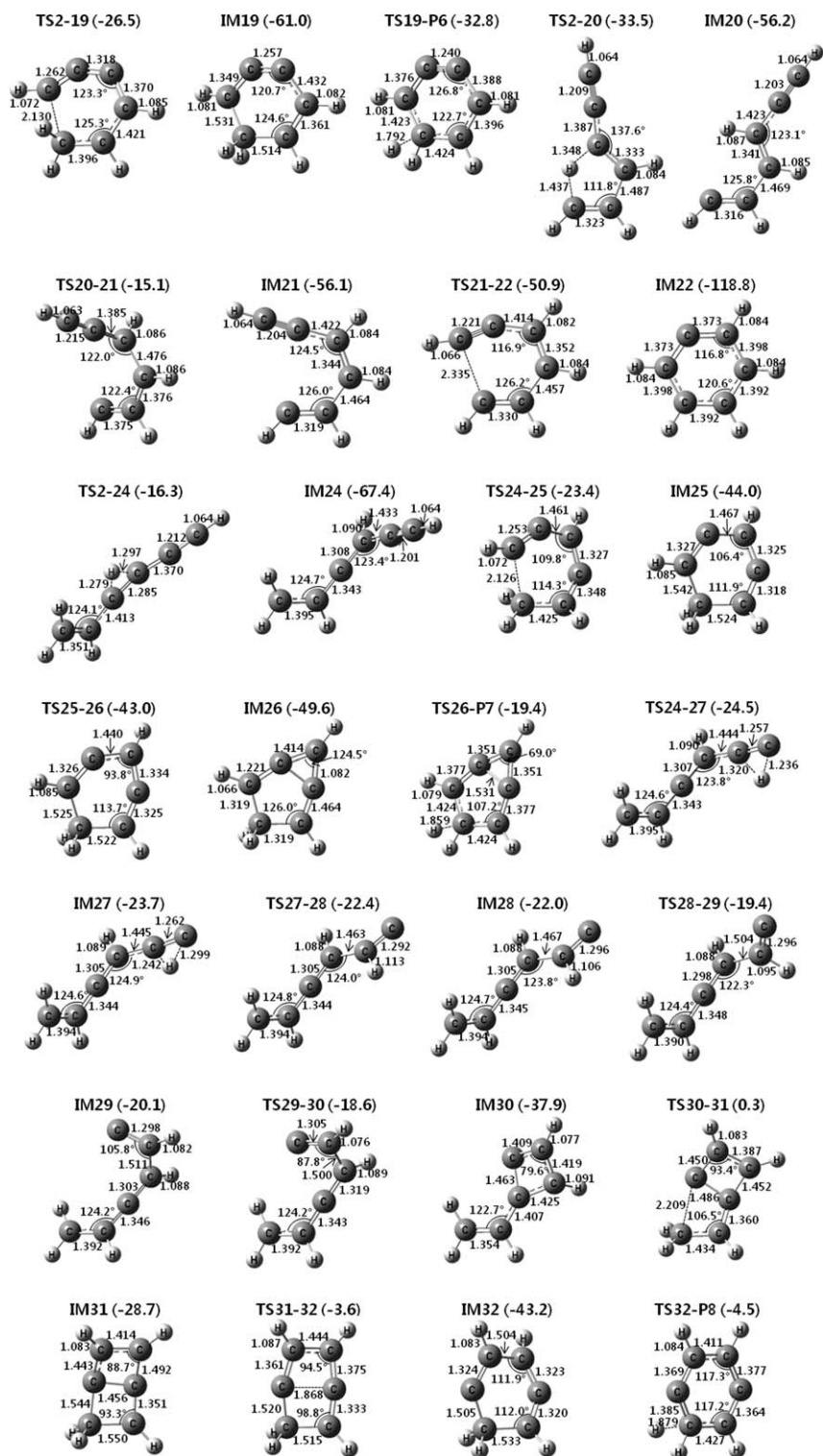
FIGURE 6. Selected parameters (bond lengths in Å and angles in degrees) of optimized structures of the transition states and the intermediates calculated by M06-2X/6-311++G(d,f) on reaction PESs of the pathways including ring formation of six-membered ring. Values in parentheses are the relative energies (in kcal/mol) calculated by CCSD(T)/6-311++G(2df,2pd)//M06-2X/6-311++G(d,f).

FIGURE 7. Reaction PESs of the pathways including ring formation of six-membered ring calculated by CCSD(T)/6-311++G(2df,2pd)//M06-2X/6-311++G(d,f). The related optimized structures are shown in Figure 6.

two terminal C atoms in the IM21 become close through the isomerization. From a low reaction barrier in the TS21-22 (5.2 kcal/mol, see Table I), the ring closing readily takes place and the IM22, thermodynamically a very stable IM, forms. The IM22 has the lowest relative energy among all IMs in the $C_4H + C_2H_4$ reaction. The reaction pathway including the IM22 is thermodynamically favorable, but it is kinetically unfavorable because of having many reaction steps and high barrier energies (detailed discussion is in the next section, Most Favorable Reaction Pathway section). All products involving a six-membered ring (P6, P7, and P8, see Fig. 1) can form through the H elimination of the IM22.

Through a migrating H atom to the next C atom in the TS2-24 (see Fig. 6, the bridged H atom is clearly shown), the IM24 forms. From the IM24, the reaction pathway branches to two products (P7 and P8, see Fig. 1). The direct ring closing occurs through the TS24-25 and then IM25 forms. Two C atoms without H atom are getting close to each other and the IM26 forms. Through the H elimination in the TS26-27, the P7 forms. Through subsequent migrating H atom from the terminal C atom to the next C atom in the IM24,

the IM27 forms. As generally a migrating H atom to the next C atom requires high reaction barrier, the reaction involving this kind of migrating is likely to be unfavorable. The calculated reaction PES between the TS27-28 and IM28 shows wrong energy order as between the TS1-3 and IM3. This result means that the reaction between the TS27-28 and IM28 may be also barrier-less process. This can be identified by the geometrical parameters of both structures; as shown in Figure 6, the geometrical parameters of both structures (TS27-28 and IM28) are almost equivalent. A *cis-trans* isomerization in the TS28-29 also makes two terminal C atoms in the IM29 be close to each other. Unlike the previous case, a six-membered ring does not form directly. First, a four-membered ring forms and subsequently a six-membered ring forms from the IM30 to the IM31. Through a breakage of the C—C bond in the IM31, the IM32 forms. Finally, H atom is detached from the ring and the P8 forms. The reaction pathway proceeding to the P8 contains many reaction steps, thus this pathway may be unfavorable.

We found a recent work on the $C_2H + C_4H_4$ reaction, which occurs on the same PES of C_6H_5

(C_4H + C_2H_4) [8]. Despite of different entrance channel, some IMs and products (including P1) are equivalent to those found in our work. One of initial adducts of the C_2H + C_4H_4 reaction (**i1** in Ref. [8]) is the same as IM24. On the C_2H + C_4H_4 reaction PES, the reaction proceeds to the IM26 (**i2** in Ref. [8]) through only one TS unlike our reaction pathway involving two TSs (TS24-25 and TS25-26). This difference may be caused by the different method (B3LYP/6-311G** method was used for geometry optimizations in Ref. [8]), but the source for this discrepancy is unclear at the moment (We cannot perform the comparison in detail because molecular structures of the transition states have not been shown in Ref. [8]). However, the energy difference (17.8 kcal/mol) between the IM24 and IM26 in our work is in excellent agreement with that (17.3 kcal/mol) of using CCSD(T)/CBS level with two-point extrapolation in Ref. [8]. The H elimination process leading to P7 (**p3**, meta-benzyne, in Ref. [8]) from the IM26 is also equivalent. The barrier and energy differences between the IM26 and P7 + H in Ref. [8] are 29.5 and 25.1 kcal/mol, respectively, which match well with those (30.2 and 24.5 kcal/mol) predicted in our work. In addition, the one of the final step leading to P6 (**p6**, *ortho*-benzyne, which is the major product in Ref. [8]) + H in Ref. [8] is equivalent to the one identified in our study. The barrier and energy differences between the IM21 and IM22 are 5.2 and 62.7 kcal/mol, respectively, which are also in excellent agreement with those (4.9 and 61.9 kcal/mol) obtained by CCSD(T)/ CBS level with two-point extrapolation in Ref. [8]. Finally, in our results, energy differences between the IM22 and P6 + H, between the P6 and P7, and between the P6 and P1 (**p1**, vinyldiacetylene, in Ref. [8]) are 78.4, 15.3, and 11.1 kcal/mol, respectively. They are in reasonable agreement with those (79.9, 14.3, and 13.8 kcal/mol) obtained by CCSD(T)/CBS level with three-point extrapolation, which is more accurate than the two-point method, in Ref. [8]. They used the most robust theoretical level, CCSD(T)/CBS with two- or three-point extrapolation methods to calculate the energetics. The close agreement of our calculated energetics results with those from such a high-level calculation confirms that the theoretical level used in our work is optimal. Moreover, the similarity of the reaction PES of C_6H_5, especially the final step leading to the products, of our work with that reported in Ref. [8], indicates that the reaction pathways found in our work are reasonable.

MOST FAVORABLE REACTION PATHWAY

As can be seen in the previous section (Pathways Including Formation of Six-Membered Ring section), numerous reaction pathways have been connected to the eight products (from P1 to P8, see Fig. 1). However, most of them have many reaction steps and high barrier energies. For example, although the IM22 has the lowest energy among all IMs (see Table I), the reaction pathway proceeding to the IM22, the final IM connecting to the P6, has four transition states (TS1-2, TS2-20, TS20-21, and TS21-22) and high reaction barrier (42.9 kcal/mol, see Table I) between the IM1 and TS1-2. On the basis of the calculated results, we propose the most favorable reaction pathway as follows:

$$C_4H + C_2H_4(C_6H_5) \rightarrow IM1 \rightarrow TS1 - P1$$
$$\rightarrow P1(C_6H_4) + H$$
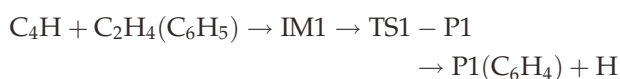
This reaction pathway has only one transition state (TS1-P1) and the reaction barrier (37.3 kcal/ mol, see Table I) is lower than that of the TS1-2. In addition, the P1 has the lowest relative energy among the chain products. In the previous experimental kinetics study for the C_4H + C_2H_4 reaction, the above reaction pathway has been assumed to occur [9]. Our calculation results support this assumption. In summary, in the most favorable reaction pathway, C_4H radical is attached to C_2H_4 and the H elimination of this adduct efficiently takes place.

Conclusions

The reaction mechanisms for the butadiynyl radical, C_4H (CCCCH), with ethylene (C_2H_4) are investigated using DFT (M06-2X) and CCSD(T) methods. The geometrical parameters and dipole moment of the $^2\Pi$ state of C_4H using M06-2X/6-311++G(d,p) are in excellent agreement with those calculated by CCSD(T)/aug-cc-pVQZ method. The reaction enthalpy (C_4H + $C_2H_4 \rightarrow$ C_6H_4 (P1) + H) calculated by CCSD(T)/6-311++G(2df,2pd)//M06-2X/6-311++G(d,f) is in excellent agreement with previously estimated value. These results indicate that the theoretical level used in this work is sufficient for calculations of this kind of hydrocarbon compounds; quite expensive theoretical level is not required. The reaction pathways of C_4H + $C_2H_4 \rightarrow C_6H_4$ + H can be categorized into three classes according

to our calculated results; (i) pathways including only chain IMs without any ring components, (ii) pathways including ring formations except the six-membered ring, and (iii) pathways including the six-membered ring. The (i) reaction pathways of $C_4H + C_2H_4$ are quite similar to those of $C_2H + C_2H_4$. In the (ii) reaction pathways, the ring closing process from the IM3 can form three four-membered ring IMs (IM7, IM8, and IM9), and they lead to various products (chain and ring) through numerous reaction steps. In the (iii) reaction pathways, $C_4H + C_2H_4$ have an enough number of C atoms to form a six-membered ring unlike $C_2H + C_2H_4$. Our results show that *cis-trans* isomerization of some chain-like IMs in the course of reaction facilitates the ring-closing process by making two terminal C atoms in C_6H_5 close to each other. On the basis of the calculated results, the most favorable reaction pathway is proposed; C_4H radical attaches to the one of C atom in C_2H_4 and the H elimination occurs with a relatively low reaction barrier to form C_6H_5 and H. This result supports the assumption made in the recent experimental kinetics study. This work may aid further experimental and theoretical investigations of astrochemical compounds and combustion processes.

References

1. Dismuke, K. I.; Graham, W. R. M.; Weltner, W. J Mol Spectrosc 1975, 57, 127.

2. Guelin, M.; Green, S.; Thaddeus, P. Astrophys J 1978, 224, L27.

3. Jamal, A.; Mebel, A. M. Phys Chem Chem Phys 2010, 12, 2606.

4. Krishtal, S. P.; Mebel, A. M.; Kaiser, R. I. J Phys Chem A 2009, 113, 11112.

5. Landera, A.; Krishtal, S. P.; Kislov, V. V.; Mebel, A. M.; Kaiser, R. I. J Chem Phys 2008, 128, 214301.

6. Landera, A.; Mebel, A. M.; Kaiser, R. I. Chem Phys Lett 2008, 459, 54.

7. Mebel, A. M.; Kislov, V. V.; Kaiser, R. I. J Am Chem Soc 2008, 130, 13618.

8. Zhang, F. T.; Parker, D.; Kim, Y. S.; Kaiser, R. I.; Mebel, A. M. Astrophys J 2011, 728, 141.

9. Berteloite, C.; Le Picard, S. D.; Balucani, N.; Canosa, A.; Sims, I. R. Phys Chem Chem Phys 2010, 12, 3677.

10. Berteloite, C.; Le Picard, S. D.; Balucani, N.; Canosa, A.; Sims, I. R. Phys Chem Chem Phys 2010, 12, 3666.

11. Dudek, R. C.; Weber, P. M. J Phys Chem A 2001, 105, 4167.

12. Ihee, H. Acc Chem Res 2009, 42, 356.

13. Ihee, H.; Lorenc, M.; Kim, T. K.; Kong, Q. Y.; Cammarata, M.; Lee, J. H.; Bratos, S.; Wulff, M. Science 2005, 309, 1223.

14. Jun, S.; Lee, J. H.; Kim, J.; Kim, J.; Kim, K. H.; Kong, Q. Y.; Kim, T. K.; Lo Russo, M.; Wulff, M.; Ihee, H. Phys Chem Chem Phys 2010, 12, 11536.

15. Kim, T. K.; Lee, J. H.; Wulff, M.; Kong, Q. Y.; Ihee, H. ChemPhysChem 2009, 10, 1958.

16. Kukura, P.; McCamant, D. W.; Yoon, S.; Wandschneider, D. B.; Mathies, R. A. Science 2005, 310, 1006.

17. Park, S. T.; Feenstra, J. S.; Zewail, A. H. J Chem Phys 2006, 124, 174707.

18. Zewail, A. H. Angew Chem Int Ed Engl 2001, 40, 4371.

19. Zheng, J. R.; Kwak, K. W.; Xie, J.; Fayer, M. D. Science 2006, 313, 1951.

20. Hohenberg, P.; Kohn, W. Phys Rev B 1964, 136, 864.

21. Kohn, W.; Sham, L. J. Phys Rev A 1965, 140, 1133.

22. Zhao, Y.; Truhlar, D. G. Theor Chem Acc 2008, 120, 215.

23. Raghavachari, K.; Trucks, G. W.; Pople, J. A.; Headgordon, M. Chem Phys Lett 1989, 157, 479.

24. Gonzalez, C.; Schlegel, H. B. J Chem Phys 1989, 90, 2154.

25. Gonzalez, C.; Schlegel, H. B. J Phys Chem 1990, 94, 5523.

26. Reed, A. E.; Curtiss, L. A.; Weinhold, F. Chem Rev 1988, 88, 899.

27. Frisch, M. J.; Trucks, G. W.; Schlegel, H. B.; Scuseria, G. E.; Robb, M. A.; Cheeseman, J. R.; Scalmani, G.; Barone, V.; Mennucci, B.; Petersson, G. A.; Nakatsuji, H.; Caricato, M.; Li, X.; Hratchian, H. P.; Izmaylov, A. F.; Bloino, J.; Zheng, G.; Sonnenberg, J. L.; Hada, M.; Ehara, M.; Toyota, K.; Fukuda, R.; Hasegawa, J.; Ishida, M.; Nakajima, T.; Honda, Y.; Kitao, O.; Nakai, H.; Vreven, T.; Montgomery, J. A., Jr.; Peralta, J. E.; Ogliaro, F.; Bearpark, M.; Heyd, J. J.; Brothers, E.; Kudin, K. N.; Staroverov, V. N.; Kobayashi, R.; Normand, J.; Raghavachari, K.; Rendell, A.; Burant, J. C.; Iyengar, S. S.; Tomasi, J.; Cossi, M.; Rega, N.; Millam, N. J.; Klene, M.; Knox, J. E.; Cross, J. B.; Bakken, V.; Adamo, C.; Jaramillo, J.; Gomperts, R.; Stratmann, R. E.; Yazyev, O.; Austin, A. J.; Cammi, R.; Pomelli, C.; Ochterski, J. W.; Martin, R. L.; Morokuma, K.; Zakrzewski, V. G.; Voth, G. A.; Salvador, P.; Dannenberg, J. J.; Dapprich, S.; Daniels, A. D.; Farkas, Ö.; Foresman, J. B.; Ortiz, J. V.; Cioslowski, J.; Fox, D. J. Gaussian 09; Gaussian, Inc.: Wallingford, CT, 2009.

28. Mccarthy, M. C.; Gottlieb, C. A.; Thaddeus, P.; Horn, M.; Botschwina, P. J Chem Phys 1995, 103, 7820.

29. Natterer, J.; Koch, W. Mol Phys 1995, 84, 691.

30. Senent, M. L.; Hochlaf, M. Astrophys J 2010, 708, 1452.

31. Sobolewski, A. L.; Adamowicz, L. J Chem Phys 1995, 102, 394.

32. Gu, X. B.; Guo, Y.; Mebel, A. M.; Kaiser, R. I. J Phys Chem A 2006, 110, 11265.